

Neutral and positively charged excitons: A magneto-optical study of a p -doped $\text{Cd}_{1-x}\text{Mn}_x\text{Te}$ quantum well

P. Kossacki

Physics Department, Institute for Micro and Optoelectronics, Swiss Federal Institute of Technology, CH1015 Lausanne, Switzerland;
Institute of Experimental Physics, Warsaw University, Hoża 69, 00-681 Warsaw, Poland;
and Laboratoire de Spectrométrie Physique, CNRS et Université Joseph Fourier-Grenoble, Boîte Postale 87,
38402 Saint Martin d'Heres Cedex, France

J. Cibert, D. Ferrand, Y. Merle d'Aubigné, A. Arnoult, A. Wasiela, and S. Tatarenko
Laboratoire de Spectrométrie Physique, CNRS et Université Joseph Fourier-Grenoble, Boîte Postale 87,
38402 Saint Martin d'Heres Cedex, France

J. A. Gaj

Institute of Experimental Physics, Warsaw University, Hoża 69, 00-681 Warsaw, Poland
 (Received 22 April 1999)

We present a systematic study of optical transitions in a modulation doped $\text{Cd}_{1-x}\text{Mn}_x\text{Te}$ quantum well with variable concentration of the hole gas. Using a semimagnetic semiconductor as the quantum well material allowed us to control independently the total hole concentration and its distribution between the two spin subbands (by a small magnetic field). Therefore, in transmission experiment we analyze population effects and distinguish the influence of spin-independent effects (screening) from spin-dependent ones (phase-space filling and intensity stealing). The observed variation of the exciton (X) and charged exciton (X^+) oscillator strengths can be accounted for assuming that the influence of phase-space filling is negligible and the variation of oscillator strength due to screening is found to be similar for both exciton species. We also show that the X^+ dissociation energy significantly increases with the population of preexisting carriers with the appropriate spin. [S0163-1829(99)09147-X]

I. INTRODUCTION

The existence of charged excitons in semiconductors was predicted long ago (1958) by Lampert.¹ The small binding energy of the additional carrier forbids the observation of these charged excitons in bulk material, but Stébé and Ainaïne pointed out in 1989 (Ref. 2) that in two-dimensional (2D) structures the binding energy should increase drastically. The observation of negatively charged excitons X^- was done by Kheng *et al.*³ in modulation doped $\text{CdTe}/\text{Cd}_x\text{Zn}_{1-x}\text{Te}$ multiple quantum wells (MQW's). This observation was rapidly followed by experimental evidence for both kinds of excitons in III-V and II-VI 2D systems.⁴⁻⁶

In this paper we report on the detailed study of the neutral exciton X and the positively charged exciton (positive trion) X^+ in a single quantum well made of a semimagnetic (diluted magnetic) semiconductor ($\text{Cd}_{1-x}\text{Mn}_x\text{Te}$). The introduction of such a material in a modulation doped heterostructure brings the new possibility of tuning the spin polarization of the carrier gas by using the so-called giant Zeeman splitting induced by a small applied magnetic field. The applied field remains small enough that the exciton wave function can be negligibly perturbed. Thus we obtain pure information about population effects.

In our experiment we utilize the same technique to control the total hole gas concentration, as for studies of the carrier-induced ferromagnetic interaction in modulation doped quantum wells.⁷ The illumination of the sample by a light of energy higher than the energy gap of the barrier allows us to

decrease the hole gas concentration, through the neutralization of holes by photo-created electrons.^{9,8} Hence, using barrier illumination and the giant Zeeman effect, we control independently the total concentration of the hole gas and the distribution of the holes between the two spin states. The total hole concentration determines spin-independent screening effects (hereafter shortened as "screening effects"), whereas varying the occupation of one of the hole spin sublevels at a constant total hole concentration should modify spin-dependent screening and phase-space filling effects. Therefore, we have a direct experimental way to distinguish the influence of screening from that of phase-space filling.

We performed a systematic study of transmission versus magnetic field under blue light illumination. We feel that the choice of transmission as the principal magneto-optical tool^{10,11} is important for the reliability of the results and their direct relationship to a model description at the present stage of knowledge. Photoluminescence (currently used in such studies for its experimental simplicity) is much more difficult to interpret since it involves not only intrinsic processes but also relaxation and competition with other recombination channels. The information obtained from reflectivity measurements, although in principle equivalent to that provided by absorption, requires usually a more precise description of the light interferences due to various dielectric interfaces in the sample and, therefore, is more difficult. Performing careful numerical fits of the absorption spectra, we analyze the oscillator strength of X and X^+ transitions and propose a simple model to describe the dependence of the intensities of

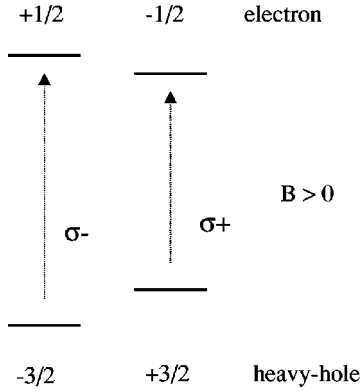


FIG. 1. Schematic diagram of optical transitions.

both X and X^+ lines on the population of each spin component of the 2D hole gas. The values of the oscillator strengths, and the efficiency of the intensity transfer from the neutral exciton to the charged exciton, are determined for vanishing hole concentration. We also show that the X^+ dissociation energy significantly increases with the population of preexisting carriers with the appropriate spin. These results should stimulate efforts toward a more complete description of the charged exciton and of its evolution to the Fermi edge singularity as the density of the 2D gas is increased.

II. SAMPLES AND EXPERIMENTAL

The present study was carried out on structures grown in a molecular-beam epitaxy chamber equipped with a home-designed electron cyclotron resonance plasma cell as a nitrogen source. Prior to fabrication of the proper samples, doping characteristics of the barrier material $\text{Cd}_{1-y-z}\text{Mg}_y\text{Zn}_z\text{Te}$ have been determined. It has been found¹² that by lowering the growth temperature down to 220–240 °C it becomes possible to reduce the nitrogen induced diffusion of Mg atoms and to obtain hole concentrations up to $5 \times 10^{17} \text{ cm}^{-3}$ in $\text{Cd}_{1-y-z}\text{Mg}_y\text{Zn}_z\text{Te}$ with $z=0.07$ and y up to 27%.

The studied modulation doped structure consists of a single 80-Å quantum well (QW) of $\text{Cd}_{1-x}\text{Mn}_x\text{Te}$ embedded between $\text{Cd}_{0.66}\text{Mg}_{0.27}\text{Zn}_{0.07}\text{Te}$ barriers grown pseudomorphically on a (100) $\text{Cd}_{0.88}\text{Zn}_{0.12}\text{Te}$ substrate. Such a layout ensures a large confinement energy for the holes in the quantum well, minimizing at the same time the effects of lattice mismatch in the thick barriers. Due to strain and confinement in the QW, the light-hole–heavy-hole splitting is of the order of 30 meV, and in the following we shall consider only heavy holes. We label the two spin subband as $+3/2$ (spin-up hole, with population p^+), and $-3/2$ (spin-down holes, with population p^-), corresponding to the normal moment of holes (not electrons) in the valence band. With this convention, a σ^+ transition involves the creation of a $-1/2$ electron and of a $+3/2$ hole; in $\text{Cd}_{1-x}\text{Mn}_x\text{Te}$, due to the giant Zeeman splitting, it occurs at lower energy than the corresponding σ^- transition (see Fig. 1).

The low Mn concentration in the QW ($x=0.0018$, see below) allows us to keep very sharp lines, but it is high enough to have a significant Zeeman splitting (~ 5 meV in a magnetic field of 5 T and at a temperature of 1.5 K). Thus we adjust the ratio p^-/p^+ from unity at zero field to practically

zero at fields of a few tenths of a tesla, at constant total population $p=p^++p^-$. Similar effects have been observed on a sample with a higher Mn content ($x=0.005$) and a slightly higher hole density.

The nitrogen doped region in the front barrier is located at a distance $L_s=200$ Å from the QW. Furthermore, in order to reduce depleting effects, two additional nitrogen doped layers reside at a distance of 1000 Å from the QW on both sides. The nominal hole concentration in the doped structure, evaluated from a self-consistent solution of the Poisson and Schrödinger equations, is $2 \times 10^{11} \text{ cm}^{-2}$. The order of magnitude of the hole density was confirmed by Hall measurements on similar structures, with the top barrier modified to allow contacting the 2D hole gas.¹³ The presence of a delocalized hole gas in the present samples was checked by photoluminescence (PL) and PL excitation (PLE). Typical spectra in magnetic field are presented in Fig. 2(a). In such a field, the spin splitting in the valence band is larger than the Fermi energy, so that the spin-down band is free of holes and an exciton can be formed between a photo-created electron and a photo-created spin-down hole.⁷ A sharp exciton line is observed in σ^- polarization [Fig. 2(a)], which will be shown below to actually be a charged exciton. A steplike PLE spectrum is observed in σ^+ polarization, as expected for an optical transition that involves the spin-up hole subband, which is partially occupied. In such spectra characteristic of a metallic system, the Moss-Burstein shift E_{MB} between the energy of PLE step and the PL maximum is generally used to evaluate the hole gas concentration. In the case of full spin polarization, we measure $E_{\text{MB}}=11$ meV, which gives [for in-plane effective masses, $m_e=0.1 m_o$ and $m_{hh}=0.25 m_o$ (Ref. 14)] a hole concentration equal to $1.6 \times 10^{11} \text{ cm}^{-2}$. This value is quite close to the one expected from the design of the structure. However, such a determination of the hole density relies on the actual value of the electron mass (and, to a lesser extent since it is larger, of the hole mass), and this determination can be altered by mass renormalization and excitonic effects.

In order to reduce the carrier concentration in the quantum well, we illuminate the barriers with additional light of controlled power and spectral characteristics (halogen lamp with a blue filter or Ar-ion laser). The mechanism of the reduction of the hole gas concentration by illumination will be discussed in Sec. III.

All magneto-optic measurements were performed in the Faraday configuration with the magnetic field applied perpendicular to the sample surface. The sample was mounted strain-free in a superconducting magnet and immersed in liquid helium. PL without additional above-gap illumination and PLE were measured using an $\text{Al}_2\text{O}_3:\text{Ti}$ laser providing about 2 mW/cm^2 . PL under illumination was measured without any further excitation than the source of light used for hole gas neutralization. The results of transmission experiments are given in the form of optical density, i.e., we plot $\ln(I_{\text{inc}}/I_{\text{trans}})$, where I_{inc} and I_{trans} are intensities of incident and transmitted light.

III. CONTROL OF THE HOLE GAS CONCENTRATION

The concentration of the hole gas is reduced by an additional illumination by light of energy higher than the energy

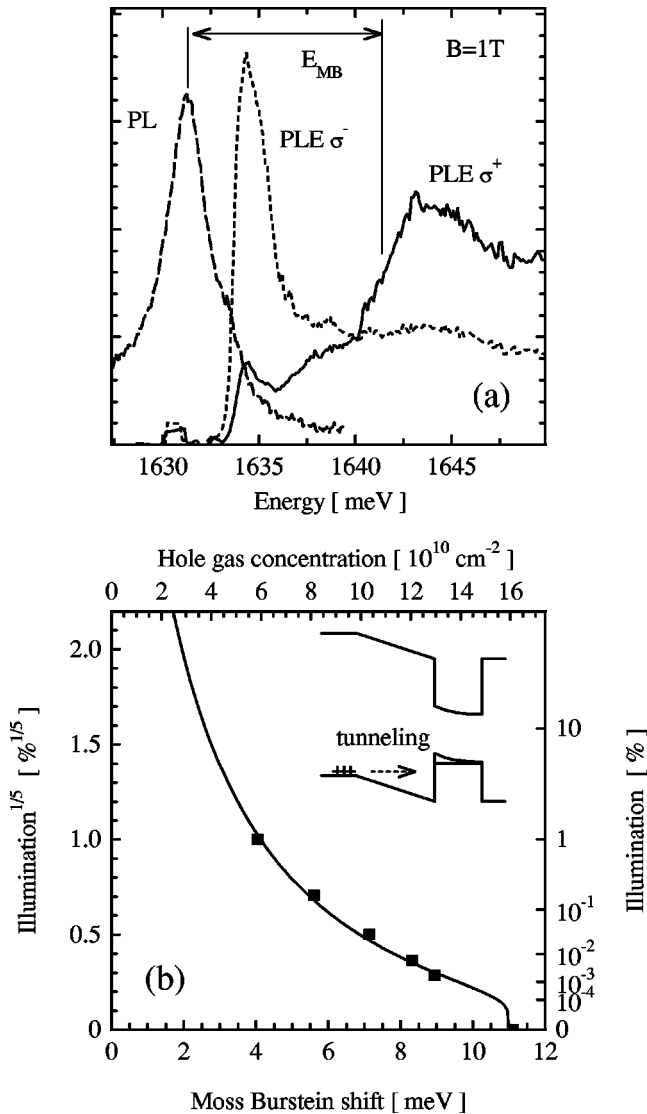


FIG. 2. Determination of the hole gas concentration in the metallic region. (a) Example spectra of PL (dashed line) and PLE (dotted line in σ^- polarization and solid line in σ^+) used to measure Moss-Burstein shift. (b) Moss-Burstein shift versus blue light illumination: The solid line represents calculation described in the text, based on tunneling across the charge-induced triangular barrier (inset). The scale (illumination intensity to the power 1/5) has no physical meaning and is used only to reduce the scale.

gap of the barrier material. The mechanism of this effect was discussed by Shields *et al.*^{5,9} and is based on the diffusion of photocreated electrons from the barrier into the quantum well where they rapidly recombine with the hole. Under continuous illumination, the system approaches a stationary state, with a reduced hole gas concentration.

In our samples the efficiency of this process was determined experimentally from the value of the Moss-Burstein shift. This shift between PLE above the Fermi energy and PL at the center of the Brillouin zone is characteristic of the metallic region at high hole density. We enhance this range by polarizing the hole gas in a small magnetic field and measuring only the σ^+ polarization, which involves the creation of a spin-up hole in the populated subband. Thanks to the giant Zeeman effect, this field remains low enough (less than 1 T) to make negligible in PL and PLE any effects

related to the quantization of the hole gas into Landau levels. The variation of the Moss-Burstein shift under moderate blue light illumination is shown in Fig. 2(b). For higher values of the illumination (i.e., for lower densities of the hole gas, below about $6 \times 10^{10} \text{ cm}^{-2}$), the character of the absorption feature changes from step-like to a well-resolved line. This is due to the excitonic effects, and this point also limits the applicability of the Moss-Burstein shift, as a source of accurate hole gas concentration. In order to estimate carrier concentrations in the range where sharp absorption lines are observed, we applied a simple model describing the neutralization of the hole gas, by the photocreated carriers.¹⁵ We assume that the current of photocreated electrons recombining in the quantum well (hence participating in the hole gas neutralization) is proportional to the illumination and that a steady state is achieved when this current balances the current of holes tunneling from the barrier into the quantum well. Therefore, the hole concentration is determined by the probability of the hole tunneling through the potential barrier between the doped region and the quantum well [inset of Fig. 2(b)]. Since the height V_0 of the triangular potential barrier is given by the hole gas concentration, if we neglect the small potential drop within the doped region, the height of the triangular barrier is $V_0 = e^2 p L_S / \epsilon \epsilon_0$, and its thickness is L_S . Hence, one obtains an approximate self-consistent equation,

$$I = \alpha(p - p_0) \exp(-\beta \sqrt{p}), \quad (1)$$

where I is the light intensity, p and p_0 are hole concentrations with and without illumination, and α and β are structure-dependent parameters defining the relation between the illumination and the electron current as well as the probability of the tunneling from the barrier into the quantum well. We expect $\beta = (8/9 m e^2 L_S^3 / \hbar^2 \epsilon \epsilon_0)^{1/2} \approx 3 \times 10^{-7} \text{ m}$ in this simple model of a triangular barrier. Actually, the parameters α and β were used as fitting parameters [see Fig. 2(b)]. We had to use $\beta = 4 \times 10^{-7} \text{ m}$, which is in reasonable agreement with this crude model. These parameters were used for the extrapolation of the hole gas concentration below the region where we can determine the carrier concentration from the Moss-Burstein shift. Our lowest hole density obtained with the halogen lamp (100% illumination) and estimated using this extrapolation is approximately $2 \times 10^{10} \text{ cm}^{-2}$. Lower hole densities were obtained with the Ar-ion laser illumination.

IV. IDENTIFICATION OF X AND X⁺ AT LOW HOLE GAS CONCENTRATION

Figure 3 shows some transmission spectra for different hole densities. Two narrow lines are well resolved at the lowest concentration displayed, $\approx 2 \times 10^{10} \text{ cm}^{-2}$. When the carrier concentration increases, the low-energy line becomes more intense while the other one weakens and finally disappears at a hole concentration of about $6 \times 10^{10} \text{ cm}^{-2}$. At the same time the lower-energy line changes its shape, and a significant broadening is observed for higher carrier concentrations. For low hole concentration, the distance between the two lines approaches 2.7 meV, i.e., the same value as that reported for the difference between the energies of exciton X and trion X⁺ in CdTe-Cd_{1-z}Zn_zMg_yTe quantum wells of similar characteristics.⁶ This finding, as well as the behavior

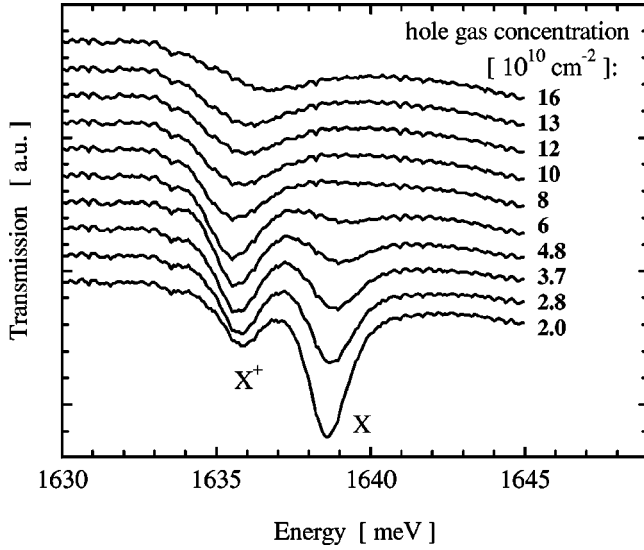


FIG. 3. Zero-field transmission spectra for different hole gas concentrations (as controlled by additional blue light illumination).

of intensities of the two lines at low hole concentrations, suggests that their origin is related to creation of neutral (X) and positively charged excitons (X^+), respectively. We expect that the presence of carriers will attenuate the neutral exciton line, due to screening and phase-space filling, while the presence of carriers, necessary for creation of charged excitons, should enhance the X^+ line with respect to the X line. A further test of this assignment can be performed by studying the influence of a magnetic field. Figure 4(a) shows transmission spectra at the lowest hole concentration, taken at several magnetic fields in both circular polarizations. We observe a characteristic population effect on the low-energy line: Its intensity increases with field in σ^- polarization, while it decreases in σ^+ . At a field of about 0.3 T, the σ^+ component disappears completely. In σ^+ polarization, the creation of a X^+ exciton in its singlet state involves a photo-created spin-up hole and a preexisting spin-down hole. Thus, this observation reflects the absence of such spin-down holes.³ Note, however, that in a $\text{Cd}_x\text{Mn}_{1-x}\text{Te}$ quantum well, the giant Zeeman effect in the conduction band leads to the same circular dichroism for the negatively charged exciton.

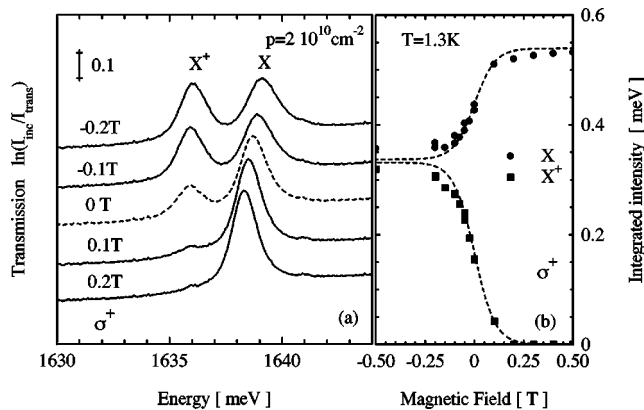


FIG. 4. Transmission (\ln of incident intensity/transmitted intensity) in magnetic field, obtained for low hole gas concentration (under 100% blue light illumination) at temperature 1.3 K: (a) spectra and (b) integrated line intensities

TABLE I. Parameters used to fit the intensity transfer at low hole density (partial hole polarization calculated with a Maxwell-Boltzmann distribution).

| Relative power of the illumination | Helium bath temperature | Spin temperature T_s | Carrier temperature T_h |
|------------------------------------|-------------------------|------------------------|---------------------------|
| 10% | 1.3 ± 0.1 K | 1.48 ± 0.1 K | 1.87 ± 0.1 K |
| 10% | 4.2 ± 0.1 K | 4.52 ± 0.1 K | 4.54 ± 0.1 K |
| 100% | 1.3 ± 0.1 K | 1.77 ± 0.1 K | 1.9 ± 0.1 K |

For an unambiguous identification, we use a quantitative test based on the fact that the giant Zeeman splitting is four times larger in the valence band than in the conduction band. First, we fit the measured exciton splitting using the phenomenological expressions given in Ref. 16 for bulk material, using the exact Mn content x as adjustable parameter and assuming that the temperature of the Mn spins T_S may be slightly higher than the nominal temperature (see Table I). A good fit is obtained for $x=0.0018$. We then analyze the intensity of both transitions by fitting two Gaussian functions to the absorption spectra. The integrated intensity of respective lines is represented versus magnetic field in Fig. 4(b). At constant total hole concentration p , we expect the intensity of the X^+ line to be roughly proportional to the population of holes with the appropriate spin, i.e., p^\pm in σ^\mp polarization, respectively. Using a Maxwell-Boltzmann distribution between the Zeeman split subbands to describe the hole concentration, we obtain for the intensity,

$$A_\pm(\Delta_z) = A(\infty) \frac{1}{1 + \exp(\mp \Delta_z / k_B T_h)}, \quad (2)$$

where Δ_z denotes the valence-band Zeeman splitting and is taken to be positive for one spin and negative for the other one, T_h is the carrier gas temperature, and k_B is the Boltzmann constant. $A(\infty)$ is the maximum intensity, achieved at total hole spin polarization. Indices + and - of the intensity denote the two circular polarizations of light. To calculate the intensity, we assume for the conduction-to-valence-band splitting the ratio 1:4, which applies for bulk heavy-hole excitons,¹⁷ and we treat the temperature of the carrier gas and the maximum intensity $A(\infty)$ as fitting parameters. Results shown in Fig. 4(b) confirm the proportionality of the X^+ intensity to the population of holes with the relevant spin. Similarly good fits are achieved at 4.2 K or at higher hole density, as shown in Fig. 5. The carrier gas temperature T_h obtained from the fit is slightly higher than the temperature of the localized spins T_S (Table I). The observed difference may be related to the fact that the sample remains under stationary conditions with a continuous diffusion of photoexcited electrons that neutralize the hole gas but may also heat the carrier gas in the quantum well. Note also that we used the Maxwell-Boltzmann distribution to describe the population ratio at low hole density where the holes are likely to be localized.^{4,18,19} The same assumption was done in Ref. 6 for a CdTe quantum well. At higher density the full Fermi-Dirac distribution should be used.

The change of the X^+ oscillator strength is accompanied by a significant change of the X exciton line intensity. This

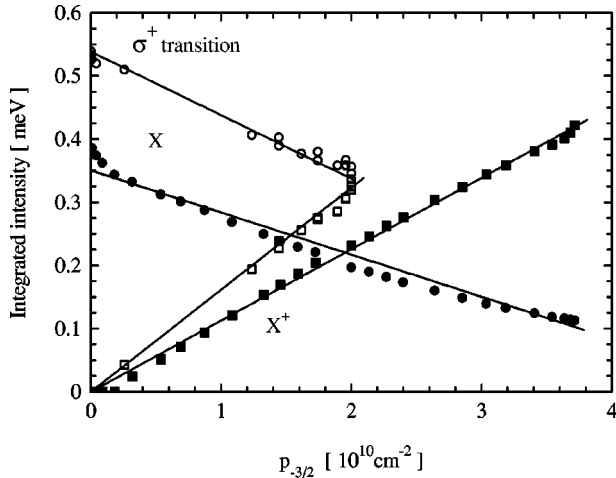


FIG. 5. Integrated intensity of transmission lines versus the hole concentration in one spin subband. Squares represent X^+ , circles X , and solid lines are a fit with Eq. (2). Total hole concentration was $2 \times 10^{10} \text{ cm}^{-2}$ (open symbols) and $3.7 \times 10^{10} \text{ cm}^{-2}$ (full symbols). The hole polarization was controlled by a magnetic field varying from -0.5 T to 0.5 T .

change can also be described by Eq. (2) with the same carrier gas temperature. Actually, the two changes are proportional to each other if the total hole population p is kept constant (see Fig. 5 and below Fig. 6). This effect cannot be explained as a result of the X line width variation as suggested in Ref. 20: As shown in Fig. 4(a), the exciton linewidth remains almost constant in the whole range of applied magnetic fields (full width at half maximum equals 2 meV). In the present sample, a broadening on the high-energy side is observed only at higher hole densities.

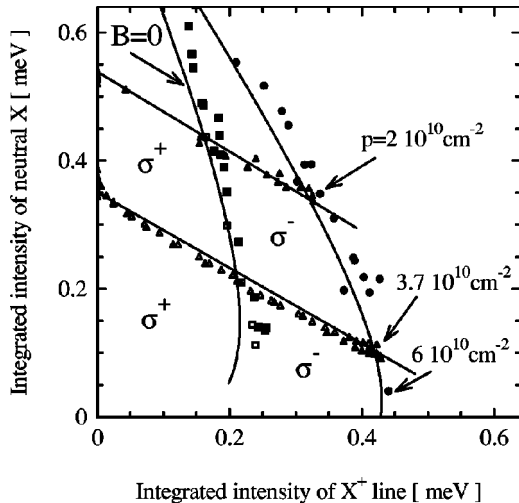


FIG. 6. Correlation between the X and X^+ intensities. Lines result from the model, full symbols are data at 1.3 K , and open symbols are data at 4.2 K . Squares are measured at zero field by varying the total hole density (blue light illumination); with respect to these data, symbols on the right (respective left) side represent data in σ^- (respective σ^+) polarization. Circles are data in σ^- polarization at complete hole polarization (corresponding data in σ^+ would sit on the vertical axis). Triangles represent magnetic field scans under constant illumination of different intensity.

V. X AND X^+ AT INCREASED CARRIER DENSITY

A. Phenomenological description of the absorption intensities

When the relevant population of holes is increased, we observe an increase of the trion intensity and a decrease of the neutral exciton intensity. To describe this opposite behavior, the idea of “intensity stealing” has been suggested,^{3,11} which could be justified by the existence of a sum rule in a closed system formed by the neutral exciton and the charged exciton. However, the total intensity (in a given polarization) is generally observed to vary as the carrier population changes, which suggests that some intensity is transferred, e.g., to band-to-band transitions. Here we can change the population of each spin subband so that we obtain complementary information.

(i) When we change the total hole density, at constant applied field, the exciton intensity decreases faster than the trion intensity increases, i.e., the sum of the two intensities decreases. This is clear on the spectra in Fig. 3 at zero field and most directly evidenced in Fig. 6, where we plot the intensity of the neutral exciton against the trion intensity.¹¹ In this plot, data at zero field (open squares at 4.2 K and full squares at 1.3 K) and data at full hole polarization in σ^- polarization (circles) both exhibit a slope higher than unity, which reflects the decrease of the summed intensity.

(ii) When we change the hole polarization at constant total density (by applying a field), it is the trion intensity that increases faster than the neutral exciton decreases. This is observed qualitatively on the spectra in Fig. 4, on the plots assuming the Maxwell-Boltzmann distribution [Figs. 4(b) and 5], and once again most directly in Fig. 6 where the data at two different hole densities (triangles) both exhibit a slope smaller than unity.

It is well known that the exciton intensity is reduced in the presence of carriers, due to various effects such as screening and phase-space filling. This reduction has been widely studied in nonmagnetic quantum wells, as a function of the total carrier density.^{11,21,22} In our phenomenological description of the transition intensities, we introduce a reduction factor $\eta(p, p_{\pm})$, for which we assume a dependence on the total carrier concentration p , regardless of its distribution between the spin subbands, and a dependence on the occupation of the valence states participating in the exciton formation, p_{\pm} .

In addition, we have to introduce the possibility of creating a charged exciton.

(i) The presence of carriers in the initial state is necessary for the creation of X^+ . It applies to the spin subband opposite to that participating in the optical transition. As a first approximation, this would make the trion oscillator strength in σ^- polarization proportional to p^+ (respectively to p^- in σ^+ polarization), see Refs. 3, 10, and 11; hence we take the oscillator strength to be proportional to $p_{\mp} \eta_{cx}(p, p_{\pm})$, where any deviation from a linear dependence on population is taken into account in the reduction factor (equal to 1 at vanishing hole densities).

(ii) The oscillator strength of the neutral exciton is reduced, and this appears to be correlated to the possibility of forming the charged exciton in the same polarization. As a first approximation, we would assume this intensity stealing^{3,11} to be proportional to the population in the rel-

evant hole spin subband, i.e., p^+ in σ^- polarization and p^- in σ^+ polarization. Hence we take

$$A_{\pm}^X(p, p_+, p_-) = A_0^X \eta_x(p, p_{\pm}) (1 - \sigma p_{\mp}) \quad (3)$$

and

$$A_{\pm}^{CX}(p, p_+, p_-) = A_0^{CX} \sigma p_{\mp} \eta_{cx}(p, p_{\pm}), \quad (4)$$

where the ‘‘cross section for intensity stealing’’ σ could depend on populations but shall be assumed to be constant. Note that we have introduced σ in the trion absorption, so that A_0^X and A_0^{CX} can be compared directly: Their ratio bears information on the extension of the wave functions in the two forms of the exciton.

The intensity effects described previously for the lowest hole concentration persist within the range of experimental conditions, where the spectra exhibit well-defined absorption lines. In particular, Fig. 5 and Fig. 6 show an identical behavior at a higher total hole density (10% illumination).

We established that to a reasonable approximation the two oscillator strengths, measured at constant total hole concentration p , are linear functions of p_{\pm} : This is clearly demonstrated in Fig. 5 for low hole density. This statement is independent of assumption of a Maxwell-Boltzmann distribution of holes on the two spin states, since we observe a doubling of the trion intensity in σ^- polarization when applying a field, with respect to the trion intensity at zero field, i.e. $\eta_{cx}(p, p_+ = p) = \eta_{cx}(p, p_+ = p/2)$. We conclude that the reduction factor $\eta_{cx}(p, p_{\pm})$ depends only on the total population and not on its distribution on the two spin states. We assume that the same is true for the neutral exciton reduction factor $\eta_x(p, p_{\pm})$. As a consequence, the two oscillator strengths become

$$A_{\pm}^X(p, p_+, p_-) = A_0^X \eta_x(p) (1 - \sigma p_{\mp}) \quad (5)$$

and

$$A_{\pm}^{CX}(p, p_+, p_-) = A_0^{CX} \sigma p_{\mp} \eta_{cx}(p). \quad (6)$$

Of course, the observed linear relation between the two oscillator strengths for a given total hole concentration follows directly from the above equations:

$$A_{\pm}^X(p, p_+) = A_0^X \eta_x(p) - \frac{A_0^X \eta_x(p)}{A_0^{CX} \eta_{cx}(p)} A_{\pm}^{CX}(p, p_+). \quad (7)$$

The parameters entering Eqs. (5) and (6) were determined on spectra with fully polarized hole gas. From the ratio of neutral exciton intensities in σ^+ and σ^- polarization, as a function of hole density [Fig. 7(a)], we obtain the cross section for intensity transfer $\sigma^{-1} = 5 \times 10^{10} \text{ cm}^{-2}$. The unscreened absorptions and the characteristic decay of screening are obtained from the plot of A_+^X and A_-^{CX} [with use of phenomenological functions $\eta_x = \exp(-p/p_x)$ and $\eta_{cx} = \exp(-p/p_{cx})$]. We obtain for the neutral exciton an unscreened intensity $A_0^X = 0.9 \text{ meV}$ and a screening with a characteristic density $p_x = 3.9 \times 10^{10} \text{ cm}^{-2}$, and for the charged exciton $A_0^{CX} = 1.3 \text{ meV}$ and a characteristic density for screening $p_{cx} = 4.7 \times 10^{10} \text{ cm}^{-2}$. Using these values, we can calculate the X intensity as a function of the X^+ intensity, not

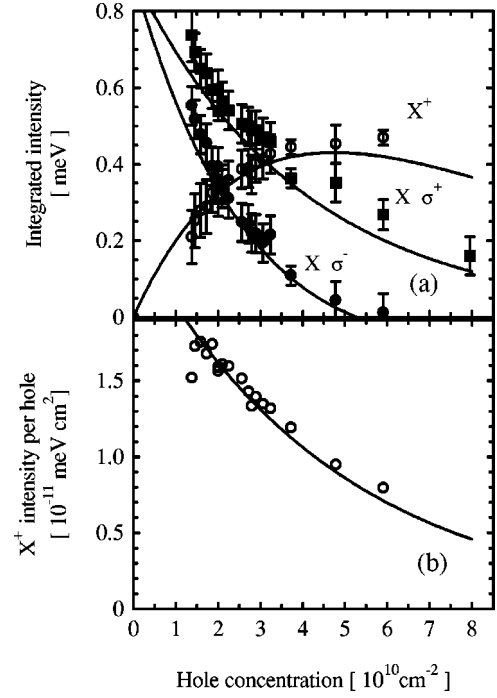


FIG. 7. Integrated intensity as a function of the hole gas concentration obtained for holes fully polarized by the magnetic field (squares, σ^+ polarization; circles, σ^- polarization). (a) Full symbols represent the X line and open symbols the X^+ line. (b) X^+ intensity per hole.

only at full polarization, but also at zero field ($p_+ = p_- = p/2$), or at constant hole density. These curves agree quite well with the experimental data (Fig. 6), showing the consistency of our empirical description.

B. Transition energy

The energies of both X and X^+ transitions as a function of the magnetic field are shown in Fig. 8 for various total hole concentrations. For the neutral exciton X , the shape of the magnetic-field dependence does not vary with hole concentration and agrees well with the modified Brillouin function.

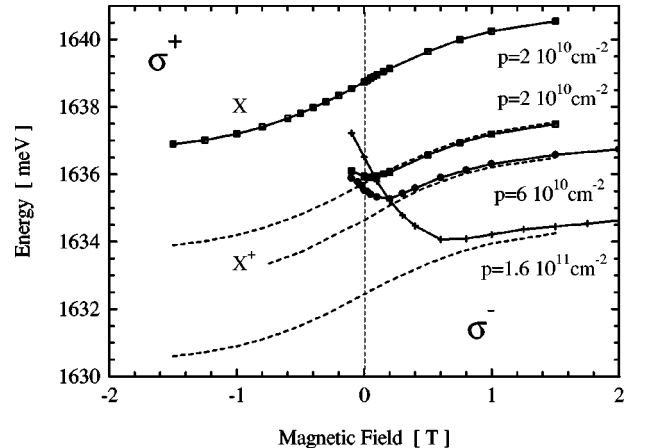


FIG. 8. Energies of the absorption lines versus magnetic field (left side, σ^+ polarization; right side, σ^- polarization), measured under different blue light illumination. Dashed lines represent the giant Zeeman effect.

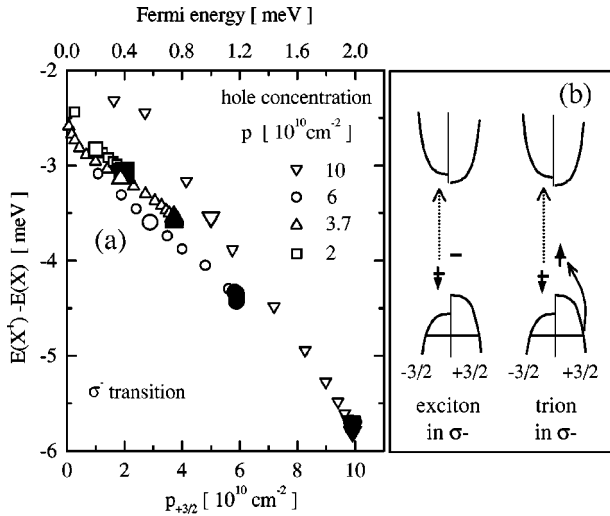


FIG. 9. (a) Charged exciton dissociation energy (difference between the X and X^+ energy) as a function of the hole gas concentration in the spin subband promoting the X^+ formation (full symbols, complete polarization of holes; big open symbols, no applied field; small open symbols, partial hole polarization calculated with a Maxwell-Boltzmann distribution). (b) Possible mechanism.

This means that no phase-space filling effects influence the X energy, in agreement with the conclusions from the oscillator strength analysis. A slight variation of the absolute values (an increase with hole concentration) should be therefore understood as an influence of screening on the exciton binding energy,^{23,24} partially balanced by band-gap renormalization and by a variation of the electrostatic potential in this asymmetric modulation doped quantum well.

Much more interesting is the dependence of the charged exciton energy. At relatively high magnetic fields in σ^- polarization, the energy of X^+ varies with field almost parallel to that of the neutral exciton, but the distance $X-X^+$ (the X^+ dissociation energy) increases linearly with the hole concentration (Fig. 9, closed symbols). An extrapolation to vanishing hole concentration gives a value of 2.5 meV. This is slightly smaller than the value 2.7 meV measured on samples with a low (but nonzero) doping.⁶ At lower field, the dissociation energy suddenly gets smaller. This appears below a characteristic field that increases with the hole density and corresponds to the field necessary to fully polarize the hole gas. If we plot the dissociation energy as a function of the population of the subband containing carriers necessary for formation of X^+ (Fig. 9), it comes out to be common for all the values of subband hole concentration. This is observed at full polarization of holes (closed symbols: $p^+ = p$, $p^- = 0$), without applied field at any total hole population (big open symbols, $p^\pm = p/2$), and at low hole density when using the Maxwell-Boltzmann distribution to calculate the hole polarization (small open symbols). The deviation observed at the maximum hole density displayed most probably indicates that the full Fermi-Dirac distribution should be used.

VI. DISCUSSION

The use of a strongly diluted magnetic semiconductor in the QW allows us to easily control the population of each

spin subband in the 2D hole gas. This is done by applying a small magnetic field—the highest field value necessary to fully polarize the hole gas at the highest hole density we use is $B = 0.6$ T, which corresponds to a magnetic length $(\hbar/qB) = 330$ Å, much larger than the exciton Bohr radius ≈ 60 Å in such a QW, and to a cyclotron energy ≈ 0.3 meV if we assume a hole mass $0.25m_0$. Hence, we can ignore any effect directly induced by the applied field, such as localization or Landau-level splitting. The only effect of the applied field is to change the relative populations of the two spin subbands. This is achieved at constant total hole density, since the Zeeman shifts in the valence band, a few meV, are more than one order of magnitude smaller than the QW depth. Thus, independently, we control the hole spin polarization and the total hole density (optically, using blue light illumination of the barriers).

At vanishing hole density, we extrapolate the integrated absorption by neutral exciton to $A_0^X = 0.9$ meV. This compares favorably with the value $2\pi\Gamma_0$, with $\Gamma_0 \approx 0.12$ meV as usually measured in similar CdTe QW's.²⁵ However, as an emissionlike signal is observed in reflectance (not shown), we would expect a constructive interference with the surface, and an enhancement of the QW absorption up to $2\pi\Gamma_0(1 - r_c)$, where the effect of surface reflectivity is introduced by the amplitude reflectivity $r_c = (1 - n_c)/(1 + n_c) \approx -0.5$ assuming a refractive index $n_c \approx 3$ for the cladding layer. We certainly underestimate the line area by choosing to fit it with a Gaussian line shape, but more appropriate line shapes (e.g., including a Lorentzian component at vanishing carrier density, or a high energy tail $\approx (\hbar\omega)^{-\alpha}$ at higher density) would be too sensitive to small, badly defined features in the wings of the line. When slightly increasing the hole density, we measure a strong intensity transfer from the neutral exciton line to the charged exciton line, in the circular polarization where it exists (both at low field, σ^- at higher field). The increase in intensity of the charged exciton line is faster than the corresponding decrease of the neutral exciton line, by a factor $A_0^{CX}/A_0^X \approx 1.5$, which bears information on the extension of the X^+ wave function. The transfer is complete for carrier densities larger than $\sigma^{-1} \approx 5 \times 10^{10}$ cm⁻², i.e., the cross section σ is characterized by a radius $\sqrt{\sigma/\pi} \approx 250$ Å much larger than the Bohr radius. It may be worth stressing that, for densities just above 6×10^{10} cm⁻², transmission (and reflectance) spectra feature a single exciton line in both polarizations, which must be attributed to the neutral exciton in σ^+ polarization and to the charged exciton in σ^- polarization.

For still higher densities, the X^+ line—not the neutral exciton—merges with the Fermi edge singularity, as already shown in the case of X^- in CdTe QW's (Refs. 26 and 27) and in GaAs QW's.^{28,4} We also demonstrate here that the excitonic feature, which appears at high density (a few 10^{11} cm⁻²) on one circular polarization when the carrier gas is fully polarized (i.e., in σ^- polarization in a p -doped Cd_xMn_{1-x}Te QW), has to be related to the charged exciton, not to the neutral exciton. Of course, this should occur also in similar cases, such as magnetoexcitons and light-hole excitons observed in the presence of a gas of heavy holes.²⁸

Quite similar screening factors $\eta(p)$, dependent on the total population, are measured here for X and X^+ . They appear at low density, much lower than expected for phase-

space filling ($1/\pi a_0 \approx 10^{12} \text{ cm}^{-2}$). It is not the aim of this paper to address this problem, but one probable source of screening in the present structure is the built-in electric field, since the QW is mainly doped on one side only.

Finally, the most appealing result of this study is the increase of the $X-X^+$ energy difference as the hole density increases. On one hand, that means that sufficient care must be taken when evaluating the binding energy of the trion and comparing to calculations that are valid in the limit of vanishing density. Our present extrapolation, 2.5 meV, is slightly smaller than the energy measured previously at small but finite energy.⁶

The observed increase of the X^+ dissociation energy with the concentration of holes with the relevant spin (preexisting carriers only) requires a deeper analysis. Theoretical results of Hawrylak and co-workers^{29,30} predict, in fact, an increase of the splitting between neutral and charged exciton, as the population increases, in the absence of spin splitting. In a simple intuitive picture, both the neutral exciton and the charged exciton are due to the existence of a bound level that appears in the 2D gas in the presence of a carrier of opposite sign (i.e., a hole in the case of an electron gas as described by Hawrylak and co-workers, an electron in the present case of a hole gas). The neutral exciton then corresponds to a single occupancy of this level. The charged exciton involves, in addition to the creation of the exciton, the transfer of a carrier of opposite spin from the Fermi level down to the bound level. If we assume that the bound level exhibits the same giant Zeeman splitting as the band, we obtain [see Fig. 9(b)],

$$E_{\pm}(X^+) = E_{\pm}(X) - \left(\frac{\hbar^2 k_{F\mp}^2}{2m^*} + E_B \right), \quad (8)$$

i.e., the $X-X^+$ splitting exhibits, in addition to the binding energy E_B , an energy proportional to the population of the subband of preexisting carriers. However, the theory described in Refs. 29 and 30 has been developed principally for an electron gas and dispersionless holes; it would need to be extended to the case where the photogenerated carrier has a finite mass (and in the present case it is smaller than the mass of the majority carriers) and to include spin splitting.

We also want to point out that very similar observations (in particular, the increase of the binding energy of the negative trion X^- and its evolution towards the Fermi edge singularity) are currently made on n -type modulation doped

CdTe-based QW's,²⁷ which calls for a coherent theoretical description of both the electron and the hole gas in such structures.

VII. CONCLUSIONS

We present a systematic study of optical transitions in a modulation doped $\text{Cd}_{1-x}\text{Mn}_x\text{Te}$ quantum well with variable concentration of the hole gas. At low hole concentrations, absorption lines due to neutral and positively charged excitons were detected. At high concentrations when the excitonic effects are eliminated by carriers, Moss-Burstein shift was used to measure the hole concentration. The data were successfully described using a simple model of carrier-concentration control by light.

Using semimagnetic $\text{Cd}_{1-x}\text{Mn}_x\text{Te}$ as the QW material, allowed us to control independently the total hole concentration (by light) and its distribution between the two spin subbands (by a small magnetic field, negligibly perturbing the electronic wave functions). Therefore, we were able to analyze population effects, as opposed to the direct influence of the magnetic field, present in most studies of similar systems. In particular, we distinguish the influence of spin-independent effects (screening) from spin-dependent ones (phase-space filling and oscillator strength stealing).

At constant total carrier density, we observe an increase of the charged exciton oscillator strength and a reduction of neutral exciton oscillator strength, both proportional to the respective subband concentration. The observed variation of the oscillator strengths can be accounted for assuming that the influence of phase-space filling is negligible and the variation of oscillator strength due to screening was found to be similar for both exciton species. While no influence of phase-space filling was found on the energy of the neutral exciton, the charged exciton dissociation energy increases linearly with the population of carriers that have the good spin to promote the trion formation in a given circular polarization.

ACKNOWLEDGMENTS

This work was partially supported by the Polish-French cooperation project "Polonium." We thank R. Cox, R. André, J-L. Staehli, V. Huard, and T. Dietl for the many long and fruitful discussions we had.

¹M.A. Lampert, Phys. Rev. Lett. **1**, 450 (1958).

²B. Stébé and A. Ainane, Superlattices Microstruct. **5**, 545 (1989).

³K. Kheng, R.T. Cox, Y. Merle d'Aubigne, F. Bassani, K. Saminadayar, and S. Tatarenko, Phys. Rev. Lett. **71**, 1752 (1993).

⁴G. Finkelstein, H. Shtrikman, and I. Bar-Joseph, Phys. Rev. Lett. **74**, 976 (1995).

⁵A.J. Shields, J.L. Osborne, M.Y. Simmons, M. Pepper, and D.A. Ritchie, Phys. Rev. B **52**, R5523 (1995).

⁶A. Haury, A. Arnoult, V.A. Chitta, J. Cibert, Y. Merle d'Aubigné, S. Tatarenko, and A. Wasiela, Superlattices Microstruct. **23**, 1097 (1998).

⁷A. Haury, A. Wasiela, A. Arnoult, J. Cibert, S. Tatarenko, T.

Dietl, and Y. Merle d'Aubigné, Phys. Rev. Lett. **79**, 511 (1997).

⁸M. Hayne, A. Usher, A.S. Plaut, and K. Ploog, Phys. Rev. B **50**, 17 208 (1994).

⁹A.J. Shields, J.L. Osborne, M.Y. Simmons, D.A. Ritchie, and M. Pepper, Semicond. Sci. Technol. **11**, 890 (1996).

¹⁰S. Lovisa, R.T. Cox, K. Saminadayar, and N. Magnea, J. Cryst. Growth **184/185**, 810 (1998).

¹¹R.B. Miller, T. Baron, R.T. Cox, and K. Saminadayar, J. Cryst. Growth **184/185**, 822 (1998).

¹²A. Arnoult, D. Ferrand, V. Huard, J. Cibert, C. Grattapain, K. Saminadayar, C. Bourgonon, A. Wasiela, and S. Tatarenko, J. Cryst. Growth **201/202**, 715 (1999).

- ¹³A. Arnoult, S. Tatarenko, D. Ferrand, J. Cibert, A. Haury, A. Wasiela, and Y. Merle d'Aubigné, *J. Cryst. Growth* **184/185**, 445 (1998).
- ¹⁴G. Fishman, *Phys. Rev. B* **52**, 11 132 (1995).
- ¹⁵E.F. Schubert and K. Ploog, *Phys. Rev. B* **29**, 4562 (1984).
- ¹⁶J.A. Gaj, W. Grieshaber, C. Bodin-Deshayes, J. Cibert, G. Feuillet, Y. Merle d'Aubigné, and A. Wasiela, *Phys. Rev. B* **50**, 5512 (1994).
- ¹⁷J.A. Gaj, R. Planel, and G. Fishman, *Solid State Commun.* **29**, 435 (1979).
- ¹⁸G. Eytan, Y. Yaon, M. Rappaport, H. Shtrikman, and I. Bar-Joseph, *Phys. Rev. Lett.* **81**, 1666 (1998).
- ¹⁹P. Gilliot, D. Brinkmann, B. Honerlage, A. Arnoult, J. Cibert, and S. Tatarenko, in *Proceedings of the 11th International Conference on Ultrafast Phenomena, Garmisch-Partenkirchen, 1998*, edited by T. Elsaesser (Springer-Verlag, Berlin, 1998), p. 254.
- ²⁰D.R. Yakovlev, V.P. Kochereshko, R.A. Suris, H. Schenk, W. Ossau, A. Waag, G. Landwehr, P.C.M. Christianen, and J.C. Maan, *Phys. Rev. Lett.* **79**, 3974 (1997); D.R. Yakovlev, V.P. Kochereshko, R.A. Suris, W. Ossau, A. Waag, G. Landwehr, P.C.M. Christianen, and J.C. Maan, *23rd ICPS, Grenoble, 1996* (World Scientific, Singapore, 1996), Vol. 3, p. 2071.
- ²¹S. Schmitt-Rink, D.S. Chemla, and D.A.B. Miller, *Adv. Phys.* **38**, 89 (1989).
- ²²M. Combescot and P. Nozieres, *J. Phys. Paris* **32**, 913 (1971).
- ²³G.D. Sanders and Yia-Chung Chang, *Phys. Rev. B* **35**, 1300 (1987).
- ²⁴A.B. Henriques, *Phys. Rev. B* **44**, 3340 (1991).
- ²⁵Y. Merle d'Aubigné, A. Wasiela, H. Mariette, and T. Dietl, *Phys. Rev. B* **54**, 14 003 (1996).
- ²⁶T. Wojtowicz, M. Kutrowski, G. Karczewski, and J. Kossut, *Appl. Phys. Lett.* **73**, 1379 (1998).
- ²⁷V. Huard, R. T. Cox, K. Saminadayar, C. Bourgoignon, A. Arnoult, J. Cibert, and S. Tatarenko (unpublished).
- ²⁸B.E. Cole, T. Takamasu, K. Takehana, R. Goldhahn, D. Schulze, G. Kido, J.M. Chamberlain, G. Gobsch, and M. Henini, *Physica B* **249-251**, 607 (1998).
- ²⁹P. Hawrylak, *Phys. Rev. B* **44**, 3821 (1991).
- ³⁰S.A. Brown, J.F. Young, J.A. Brum, P. Hawrylak, and Z. Wasilewski, *Phys. Rev. B* **54**, R11 082 (1996).